Mapping and manipulating temperature–concentration phase diagrams using microfluidics†

Šeila Selimović,[a] Frédéric Gobeaux[b] and Seth Fraden*[a]

Received 7th December 2009, Accepted 10th March 2010
First published as an Advance Article on the web 20th April 2010
DOI: 10.1039/b925661j

We describe a microfluidic device for mapping phase diagrams of aqueous samples as a function of concentration and temperature. This double-layer (poly)dimethylsiloxane (PDMS) device contains a storage layer, in which hundreds of nanolitre sized aqueous droplets can be simultaneously formed and stored. A second layer, separated by a thin, water-permeable PDMS-membrane contains twelve reservoir channels filled with different salt solutions. When there is a difference between the concentrations of salt in the reservoir solutions and the aqueous droplets, water migrates across the membrane and causes the droplets to reversibly shrink or expand and the concentration of all solutes inside the droplets changes. We now incorporate a temperature stage that generates a linear gradient in temperature across the chip oriented perpendicular to the concentration gradient. Robust operation of several variants of the PhaseChip is demonstrated with examples in liquid–liquid phase separation and protein crystallization experiments.

Introduction

In the past few years there has been a concerted effort in the microfluidics community to design new tools for studying protein crystallization and the phase behavior of aqueous solutions.[1–9] The main advantages of microfluidic devices for these applications are a reduction in volume of the costly proteins needed to run a crystallization screen and the increased control over the physical parameters affecting phase transitions. Previously, with a device we refer to as the PhaseChip,[7] we have shown that manipulating the osmotic pressure of the solution is an effective way to control the solute supersaturation, for example in order to decouple crystal nucleation from crystal growth.[6,7] Temperature, however, is also a key parameter that affects supersaturation.[10,11,12] In this paper we report the capabilities of a new generation of the PhaseChip, which combines control over solute concentration with temperature control and enables us to measure the concentration and temperature dependent phase diagram of proteins and other aqueous solutions. Additionally, we can conduct hundreds of protein crystallization screens simultaneously, while still consuming a small amount of solute.

The PhaseChip refers to a class of bi-layer (poly)-dimethylsiloxane (PDMS) microfluidic devices for phase studies of polymers and proteins. In one device, the upper layer contains over 792 aqueous droplets stored in 20 nl wells. Another device, designed for high throughput crystallization and phase transition experiments, can store 5040 emulsion droplets in 65 pl wells (see ESI†). We refer to the two devices as the "20 nl PhaseChip" and "emulsion PhaseChip", respectively (see ESI† for experiments conducted using the "emulsion PhaseChip"). The bottom layer of the PhaseChip is the same for both devices and contains reservoir channels through which salt solutions flow continuously. The well and the reservoir layer are separated by a thin membrane of PDMS, which is only permeable to water, but not to polymer, protein or salt. In our experiments the droplets and the reservoir solutions initially contain different concentrations of salt, and the resulting difference in chemical potential of water inside the reservoir and inside a drop drives the flow of water across the membrane. Depending on the sign of this gradient, water flows either into the drops, thereby swelling them and lowering the solute concentration, or out of the drops, therefore shrinking them and raising the solute concentration. Either process is reversible. Note that as a droplet changes size, the

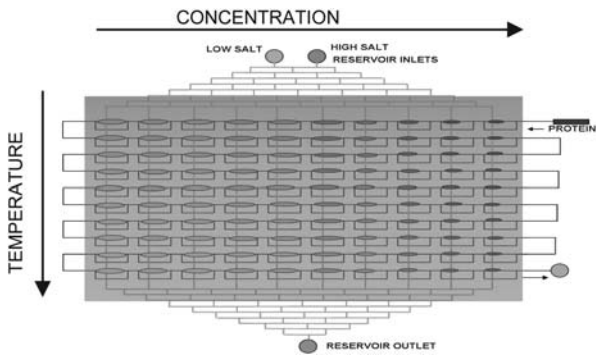

Fig. 1 Schematic of the concentration and temperature gradients on the PhaseChip. When two different salt solutions are introduced into the reservoir (low salt and high salt), a discrete linear gradient of salt concentration forms across the reservoir channels (in this sketch, the salt concentration increases to the right). Superposed on the concentration gradient is a continuous linear temperature gradient. Directions of both gradients are reversible. (For more information see ESI†).

[a]*Martin Fisher School of Physics, Brandeis University, 415 South Street, Waltham, MA, 02453, USA. E-mail: fraden@brandeis.edu; Fax: +1 781 736 2915; Tel: +1 781 736 2888*
[b]*iBiTec-S/SB2SM CEA et CNRS URA 2096, CEA-Saclay, F-91191 Gif-sur-Yvette, France*

† Electronic supplementary information (ESI) available: Device structure, experimental setup, phase diagram measurements of PEG/salt, crystallin and lysozyme, movie of protein crystallization and PDF of chip masks. See DOI: 10.1039/b925661j

concentrations of protein, precipitant, buffer, and polymer within the same drop are coupled and hence change accordingly.

The reservoir has a tree-like structure, originally developed by Jeon *et al.*:[13] two fluids of different salt concentrations (*e.g.* high concentration and low concentration salt solution) enter the reservoir independently, then as the flows branch through the tree-like channel structure, their contents mix *via* diffusion and finally separate into twelve distinct streams, where salt concentration varies linearly from stream to stream. This gives rise to a one-dimensional spatial gradient of salt concentration across the reservoir channels, which in turn controls the solute concentration inside the droplets and thus generates a concentration gradient across the droplets stored on-chip. In operation, the PhaseChip is loaded with drops of identical solute concentration, eliminating the need for complex drop formulation elements. As the experiment progresses and the drops "equilibrate" with the reservoir, their concentration changes, leading to drops of high solute concentration on one side of the chip and low solute concentration on the other side (Fig. 1).[7]

The PhaseChip allowed us to reversibly vary the solute concentrations inside the droplets by changing the concentration of the reservoir salt solutions, leading to multiple cycles of supersaturation per sample in a closed device. Most microfluidic systems capable of regulating the solute concentration do not offer such wide range of control: The crystallization system developed by Quake *et al.*[2,8] utilizes free interface diffusion, and the approach taken by Ismagilov[1,9] relies on microbatch droplets, so neither method is reversible. Microfluidic phase and crystallization studies based on temperature quenches, like in the case of Salmon *et al.*,[12] are reversible, but there is no on-chip control over the solute concentrations.

In addition to this concentration control, the PhaseChip is placed on a thermal stage, in which a temperature gradient is generated by placing two independent thermoelectric coolers at opposite ends of a thin metal plate (Fig. S2†). The PDMS device is positioned such that the direction of the temperature gradient is perpendicular to the concentration gradient (Fig. 1). In effect, the PhaseChip now displays a two-dimensional phase diagram of the solutes in question, with each position on the chip corresponding to a particular value of concentration and temperature. Hence, any phase change observed in the droplets can be assigned to quantitative values of temperature and solute concentration during the experiment. This information can then be used to readily adjust experimental parameters in order to either independently expand or reduce the temperature or concentration range.

Experimental section

The PhaseChip (Sylgard 184 PDMS, Dow Corning) can store 792 aqueous drops of 20 nl volume ("20 nl PhaseChip"), or 5040 emulsion drops of 65 pl ("emulsion PhaseChip", see ESI†) in individual wells. The storage region is 2 cm × 4 cm in size for both devices. In both PhaseChip designs the drops are separated by fluorinated oil, such that they are physically and chemically isolated from each other and represent independent experiments. The oil is pumped constantly through the storage region at 10 μl h^{-1} in order to compensate for the change in volume as the drops shrink. Details of PhaseChip manufacture and of drop formation and storage are in the ESI†.

The temperature stage is fabricated from brass, with two embedded thermoelectric coolers (TEC, Melcor PT4-7-30) that can be controlled independently by two PID circuits (Analog Devices, EVAL-ADN8831). These are in turn operated *via* a LabView interface, thereby allowing us to create a temperature gradient across the long side of the PhaseChip storage region (Fig. S2†). On this concentration–temperature gradient grid, where the two control parameters are perpendicular to each other, several droplets are exposed to the same combination of concentration and temperature, because our reservoir design is limited to twelve different concentrations per chip. However, the number of different temperatures is set by the number of storage rows (33 for the 20 nl chip and 90 for the emulsion chip). While there are several hundred distinct and simultaneous experiments on each version of the PhaseChip (396 and 1080 for the 20 nl and emulsion chips, respectively), the built-in redundancy in physical conditions serves to check the reproducibility of the phase behavior.

In all the experiments the drops initially introduced into the PhaseChip are identical. Typically it takes twelve hours for the drops to reach a steady-state concentration and two minutes to reach a steady state in temperature. Drops are monitored with an automated 3-axis microscope stage with a 4× objective lens and a resolution of 10 μm. We typically record images of the aqueous drops every 15 minutes. This allowed us to measure the size of the drops and thus determine changes in solute concentrations over time and also to record any phase changes.[7] We demonstrate the operation of the PhaseChip in protein crystallization with a quorum–quenching protein AiiB(S35E). Other examples are discussed in the ESI†: (I) polymer–salt liquid–liquid coexistence curve, (II) eye-lens protein liquid–liquid coexistence, and (III) protein crystallization with lysozyme.

Screening protein crystallization conditions for *N*-acyl-L-homoserine lactonase AiiB(S35E)

The protein drops used in our PhaseChip experiment contain the following components: 5 mg ml^{-1} protein in 10 mM 4-(2-hydroxyethyl)-1-piperazineethanesulfonic acid (HEPES) at pH 7.5 and 0.55 M ammonium tartrate ($(NH_4)_2C_4H_4O_6$) at pH 7.5. The reservoir is fed with 0.5 M and 1.5 M ammonium tartrate solutions. A temperature gradient between 12 °C and 31 °C is imposed for the duration of the experiment.

Results

The *N*-acyl-L-homoserine lactonases (AHL lactonase) are enzymes that block bacterial cell–cell communication.[14] An AHL lactonase from *Agrobacterium tumefaciens*, AiiB, has been crystallized and its structure determined. Here we report a crystallization condition without phosphate, known to block the active site, for a mutant protein AiiB(S35E) in which the residue serine 35 has been mutated to a glutamate. Previous crystallization tests[15] conducted in crystallization plates on microlitre sized drops determined conditions that yield many crystals. The PhaseChip consumes 1000 times less protein per crystallization trial, however, making it possible to conduct more trials and scan

a wider concentration and temperature space than previously possible in order to find the condition appropriate for growing a single large crystal per drop.

First protein crystals under the PhaseChip conditions described in the Experimental section are observed after a period of 24 hours. Visual inspection of the PhaseChip indicates clearly delineated regions of the device that contain clear (stable) drops, drops in which the protein and precipitant have undergone liquid–liquid phase separation, and a wide crystallization region (Fig. 2a). We note that there are two crystal morphologies present (elongated and compact, which we did not characterize further) and a distinct region on-chip where each drop contains exactly one crystal. The corresponding phase diagram is shown in Fig. 2b.

Conclusions

We have demonstrated the versatility of the PhaseChip for the quantitative mapping of phase diagrams and for the kinetic manipulation of thermodynamic variables to influence phase behavior. In a typical experiment, the PhaseChip consumes 2 μl of solution and controls simultaneously up to 1000 different conditions in the concentration–temperature plane. The PhaseChip offers excellent and reversible control over the concentration of all solutes inside test droplets. In our experiments, concentrations across a chip typically vary by a factor of 2 (Fig. 2, ESI†). Thermoelectric coolers provide excellent spatial and temporal control of temperature across the full device and the PhaseChip performs equally reliably whether the temperature across the chip is constant or a large spatial temperature gradient is applied, for example in the range of 2 °C to 40 °C.

We dynamically follow the progression of concentration changes in all drops stored on-chip. Thus, a visual inspection of the droplets with a microscope allowed us to quantitatively evaluate an experiment before its completion, and adjust the experimental parameters to achieve a desired temperature and concentration range on-chip. This feedback control, combined with reversible regulation of both concentration and temperature, is, to our knowledge, novel in the area of high throughput microfluidic devices, and especially in microfluidics based protein crystallization.

The performed experiments demonstrate that the PhaseChip can be used to study a variety of problems, from quantitative determination of phase diagrams in protein solutions to protein crystallization screens. In our study of the protein AiiB(S35E) we have shown that a concentration–temperature crystallization screen led to an optimal condition that yields exactly one large crystal per drop, rather than many small ones, which is of interest to crystallographers, who rely on large and well-ordered crystals to extract structural data.

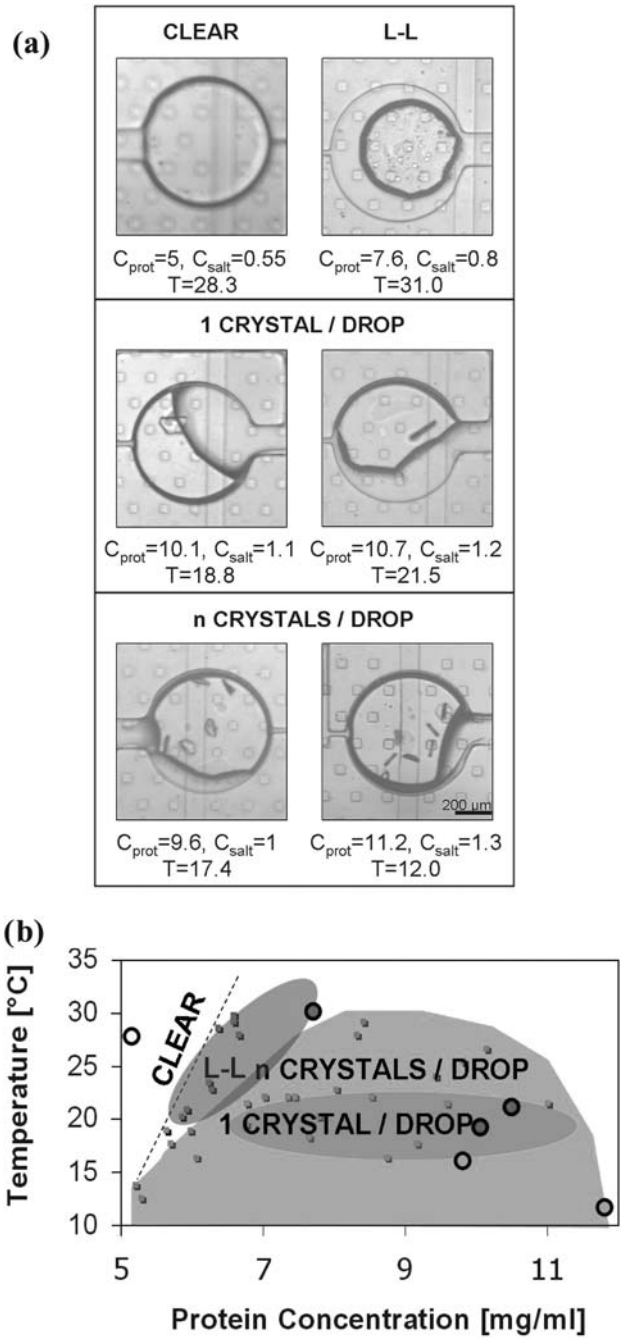

Fig. 2 (a) Sample images from the AiiB crystallization screen, taken 31 hours after beginning the experiment. Different phases are observed. Scale bar is 200 μm. Salt concentration (C_{salt}) is in mM, protein concentration (C_{prot}) is in mg ml^{-1}, and temperature (T) is in °C. (b) Phase diagram of the bacterial lactonase AiiB. We only report the protein concentration, but it is coupled with the salt concentration. Four distinct regions are apparent in this diagram: clear drops (left of the dashed line), liquid–liquid phase separated region (L–L), one crystal per drop, and several crystals per drop. The filled circles show the data from the photographs in (a).

Acknowledgements

We thank Ryan Whelan for building the temperature stage; Professor George Thurston (Rochester Institute of Technology) for providing us with purified bovine γB crystallin samples; Dr Walter Fast and Dr Pei W. Thomas (University of Texas, Austin) for supplying the AiiB protein samples; Dr Dali Liu (Brandeis University) for conducting AiiB off-chip crystallization trials;

RainDance Technologies for providing the non-ionic triblock surfactant. We acknowledge support from the Brandeis NSF MRSEC—0820492 and NSF IDBR—0754769.

References

1 C. J. Gerdts, V. Tereshko, M. K. Yadav, I. Dementieva, F. Collart, A. Joachimiak, R. C. Stevens, P. Kuhn, A. Kossiakoff and R. F. Ismagilov, *Angew. Chem., Int. Ed.*, 2006, **45**(48), 8156–8160 andC. J. Gerdts, M. Eliott, S. Lovell, M. B. Mixon, A. J. Napuli, B. L. Staker, P. Nollert and L. Stewart, *Acta Crystallogr., Sect. D: Biol. Crystallogr.*, 2008, **64**, 1116–1122.

2 C. L. Hansen, E. Skordalakes, J. M. Berger and S. R. Quake, *Proc. Natl. Acad. Sci. U. S. A.*, 2002, **99**, 16531–16536.

3 J. Leng and J.-B. Salmon, *Lab Chip*, 2009, **9**, 24–34.

4 S. L. Perry, G. W. Roberts, J. D. Tice, R. B. Gennis and P. J. A. Kenis, *Cryst. Growth Des.*, 2009, **9**, 2566–2569.

5 K. Dhouib, C. K. Malek, W. Pfleging, B. Gauthier-Manuel, R. Duffait, G. Thuillier, R. Ferrigno, L. Jacquamet, J. Ohana, J. L. Ferrer, A. Theobald-Dietrich, R. Giege, B. Lorber and C. Sauter, *Lab Chip*, 2009, **9**, 1412–1421.

6 Š. Selimović, Y. Jia and S. Fraden, *Cryst. Growth Des.*, 2009, **9**(4), 1806–1810.

7 J. U. Shim, G. Cristobal, D. R. Link, T. Thorsen, Y. W. Jia, K. Piattelli and S. Fraden, *J. Am. Chem. Soc.*, 2007, **129**, 8825–8835.

8 C. Hansen and S. Quake, *Curr. Opin. Struct. Biol.*, 2003, **13**, 538–544.

9 H. Song, D. L. Chen and R. F. Ismagilov, *Angew. Chem., Int. Ed.*, 2006, **45**, 7336–7356.

10 O. Galkin and P. Vekilov, *J. Phys. Chem. B*, 1999, **103**, 10965–10971.

11 J. R. Luft, J. R. Wolfley, M. I. Said, R. M. Nagel, A. M. Lauricella, J. L. Smith, M. H. Thayer, C. K. Veatch, E. H. Snell, M. G. Malkowski and G. T. DeTitta, *Protein Sci.*, 2007, **16**, 715–722.

12 P. Laval, A. Crombez and J.-B. Salmon, *Langmuir*, 2009, **25**, 1836–1841.

13 N. L. Jeon, S. K. W. Dertinger, D. T. Chiu, I. S. Choi, A. D. Stroock and G. M. Whitesides, *Langmuir*, 2000, **16**(22), 8311–8316.

14 M. R. Parsek and E. P. Greenberg, *Proc. Natl. Acad. Sci. U. S. A.*, 2000, **97**, 8789–8793.

15 D. Liu, P. W. Thomas, J. Momb, Q. Q. Hoang, G. A. Petsko, D. Ringe and W. Fast, *Biochemistry*, 2007, **46**, 11789–11799.